HHS Public Access

Author manuscript

Neuroscience. Author manuscript; available in PMC 2016 July 22.

Published in final edited form as:

Neuroscience. 2016 July 22; 328: 1–8. doi:10.1016/j.neuroscience.2016.04.023.

NEURONATIN IS A STRESS-RESPONSIVE PROTEIN OF ROD PHOTORECEPTORS

VISHAL SHINDE[†], **PRIYAMVADA M. PITALE**[†], **WAYNE HOWSE**, **OLEG GORBATYUK**, and **MARINA GORBATYUK**[*]

University of Alabama at Birmingham, Department of Optometry, United StatesUniversity of Alabama at Birmingham, Department of Vision Science, School of Optometry, United States

Abstract

Neuronatin (NNAT) is a small transmembrane proteolipid that is highly expressed in the embryonic developing brain and several other peripheral tissues. This study is the first to provide evidence that NNAT is detected in the adult retina of various adult rod-dominant mammals, including wild-type (WT) rodents, transgenic rodents expressing mutant S334ter, P23H, or T17M rhodopsin, non-human primates, humans, and cone-dominant tree shrews. Immunohistochemical and quantitative real time polymerase chain reaction (qRT-PCR) analyses were applied to detect NNAT. Confocal microscopy analysis revealed that NNAT immunofluorescence is restricted to the outer segments (OSs) of photoreceptors without evidence of staining in other retinal cell types across all mammalian species. Moreover, in tree shrew retinas, we found NNAT to be co-localized with rhodopsin, indicating its predominant expression in rods. The rod-derived expression of NNAT was further confirmed by qRT-PCR in isolated rod photoreceptor cells. We also used these cells to mimic cellular stress in transgenic retinas by treating them with the endoplasmic reticulum stress inducer, tunicamycin. Thus, our data revealed accumulation of NNAT around the nucleus as compared to dispersed localization of NNAT within control cells. This distribution coincided with the partial intracellular mislocalization of NNAT to the outer nuclear layer observed in transgenic retinas. In addition, stressed retinas demonstrated an increase of NNAT mRNA and protein levels. Therefore, our study demonstrated that NNAT is a novel stress-responsive protein with a potential structural and/or functional role in adult mammalian retinas.

Keywords

neuronatin; retinal degeneration; rod photoreceptors; autosomal dominant retinitis pigmentosa; ER stress

[*]Correspondence to: M. Gorbatyuk, Department of Vision Sciences, University of Alabama at Birmingham, 1670 University Boulevard, Birmingham, AL 35233, United States. Tel: +1-205-934-6762; fax: +1-205-934-3425., ; Email: mgortk@uab.edu (M. Gorbatyuk)

[†]Authors contributed equally.

DISCLOSURES

The authors declare no conflict of interest

INTRODUCTION

The retina is a specialized neuronal tissue that plays a vital role in vision. The structural and functional integrity of the retina is supported by the coordinated work of six types of neurons and glial cells. All retinal neurons express a unique protein signature that defines their roles in the functioning of the whole retina. Thus the photoreceptor cells express opsin, a key protein of phototransduction; retinal pigment epithelium cells express pigment epithelium-derived factor, a multifunctional protein promoting photoreceptor survival and supplying the retina with anti-angiogenic action; ON and bipolar cells express glutamate receptor proteins, allowing them to provide a distinct response to the release of glutamate in transmitting a signal from the photoreceptors to the ganglion cells. Despite the recent breakthrough in retinal functional proteomics, many key regulators of the vision process remain to be identified and their function remains to be characterized.

The downstream target of NeuroD1, neuronatin (NNAT), is a proteolipid (Dou and Joseph, 1996) that originally was discovered as a gene involved in the development and differentiation of the central nervous system (Chu and Tsai, 2005). Later, its expression was detected in other non-neuronal adult tissues (Dugu et al., 2010). In humans, the imprinted NNAT gene is expressed only as a paternal allele (Joseph et al., 1994, 1995; Wijnholds et al., 1995) encoding two major isoforms. NNAT-α encodes an 81-aa protein that arises from exons 1, 2, and 3 while NNAT-β encodes a 54-aa protein that originates from the first and the third exons. The proteins encoded by the α and β isoforms have distinct peaks of accumulation during brain development (Joseph et al., 1995; Siu et al., 2008). Thus NNAT-α is expressed earlier than NNAT-β, suggesting different regulatory mechanisms governing their expression. While highly expressed during development, NNAT expression subsequently declines in the adult brain (Joseph et al., 1994; Usui et al., 1996). In the retina, a study demonstrated NNAT mRNA expression at postnatal day (P) 0 and its consequent decline in adult retinas (Dorrell et al., 2004). Despite this significance, the above-mentioned study did not reveal the precise localization of NNAT in different retinal neurons.

In addition to the developing brain, the expression of NNAT has also been reported in the pituitary gland, lungs, adrenal gland, uterus, skeletal muscle, ovaries, pancreas, and skin (Wijnholds et al., 1995; Niwa et al., 1997; Arava et al., 1999; John et al., 2001). These reports have highlighted different patterns of expression of the NNAT isoform. Thus the reduction of NNAT-α was observed in the β-cells of diabetic rodents (Chu and Tsai, 2005; Joe et al., 2008), while the endothelial cells of blood vessels in obese and diabetic mice showed increased levels of NNAT-α (Mzhavia et al., 2008). All these findings indicate potentially different roles for NNAT isoforms in development and during adulthood.

As of today the precise role of NNAT in healthy and diseased adult human tissues has not been addressed. Thus, Zheng et al. have proposed the protective role for NNAT during neuronal development from the external toxic insults (Zheng et al., 2002), while other studies conducted with non-neuronal cells suggested that NNAT could act as an intracellular Ca^{2+} modulator (Suh et al., 2005; Poon et al., 2006; Joe et al., 2008). In addition to maintaining cellular homeostasis, NNAT can play a role in pathological processes. Thus in patients with glioblastoma, the elevated NNAT level is associated with poor prognosis and

serves as a prognostic biomarker (Xu et al., 2012) while in patients with prostate cancer, NNAT suppression is involved in the mechanism of metformin-induced apoptosis in cells (Yang et al., 2015). Recently, Mzhavia et al. have also described the pathophysiological role of NNAT in diabetic vascular disease and have demonstrated NNAT-induced upregulation of NF-kB, increase in inflammatory gene expression, and the promotion of p38 and Jun-N signaling molecules in endothelial cells (Mzhavia et al., 2008). In patients with Lafora disease, NNAT has been reported to contribute to neuro pathogenesis by mediating aberrant Ca^{2+} signaling, the activation of endoplasmic reticulum (ER) stress, and the formation of aggregates called Lafora bodies (Sharma et al., 2013).

All these reports have indicated that NNAT could be one of the key molecules that maintain cellular homeostasis. However, although the potential role of NNAT in several organs and tissues has been highlighted, no comprehensive study has been conducted to examine the role of NNAT in developing and adult retinas. This fact demonstrates the gap in the knowledge of the retinal proteome affecting our comprehensive concepts of retinal physiology. Therefore we initiated a study of NNAT in which we analyzed the expression and localization of the NNAT protein in the mammalian retinas of a wide spectrum, ranging from mice to humans. Using quantitative real time polymerase chain reaction (qRT-PCR), western blot and Immunohistochemical (IHC) analyses, we detected NNAT in adult retinas and additionally revealed that the intercellular localization of NNAT could differ in healthy and diseased adult retinas.

EXPERIMENTAL PROCEDURES

Animal models

The animal protocol was carried out with approval from the Institutional Animal Care and Use Committee at the University of Alabama at Birmingham and in accordance with the guidelines of the Association for Research in Vision and Ophthalmology statement for the use of Animals in Ophthalmic and Vision Research. All efforts were made to minimize the number and the suffering of the animals used.

Homozygous S334ter Rho (line 4), P23H Rho (line 3) transgenic rats, and C57/BL6 rhodopsin knockout and T17M RHO mice were maintained in the UAB housing facility. Heterozygous transgenic rats were bred with wild-type (WT) Sprague–Dawley (SD) rats to generate heterozygous S334ter-4 Rho and P23H-3 Rho rats. The T17M RHO mice were bred with C57/BL6 mice to generate heterozygous T17M RHO mice.

RNA preparation and real-time PCR analysis

Retinas from SD and S334ter-4 Rho rats were isolated at postnatal day (P) 21, P40 and P60. Total RNA was isolated from the individual retinas from each strain using Trizol (n=5). cDNA was prepared using a cDNA reverse transcription kit (Applied Biosystems) from the RNA extracts of SD and S334ter-4 Rho retinas. Each cDNA (20 ng) was subjected to qRT-PCR using Applied Biosystems TaqMan assays (validated for each selected gene) on a One Step Plus instrument (Applied Biosystems, Foster City, CA, USA) to compare the number of

cycles (Ct) needed to reach the midpoint of the linear phase. All observations were normalized to the GAPDH housekeeping gene.

Western blot analysis

The retinal protein extract was obtained from SD, S334ter and P23H Rho rats by sonication in a buffer containing 25 mM of sucrose, 100 mM of Tris–HCl, pH=7.8, and a mixture of protease inhibitors (PMSF, TLCK, aprotinin, leupeptin, and pepstatin). The total protein concentration in the right and left retinas from individual rats were measured using a Biorad protein assay, and 40–60 μg of total protein was used to detect individual proteins. The detection of proteins was performed using an infrared secondary antibody and an Odyssey infrared imager (LiCor Inc., Lincoln, Nebraska, USA). The NNAT antibody from abcam (Cat # ab27266) was used at a dilution of 1:1000.

IHC analysis

Rats and mice were euthanized separately using a CO_2 chamber. The eyeballs were enucleated, affixed in 4% freshly made paraformaldehyde (Cat# S898-09 J.T. Baker, Phillipsburg, NJ, USA), and kept at 4 °C for 8 h. Then, the eyes were hemisected and the eyecups were transferred to fresh phosphate-buffered saline (PBS) to remove formaldehyde, and then immersed in a 30% sucrose solution for cryoprotection. Eyecups were then embedded in a cryostat compound (Tissue TEK OCT, Sakura Finetek USA, Inc., Torrance, CA, USA) and frozen at −80 °C. Twelve-micron sections were obtained using a cryostat. Twelve-micron sections of rat (SD and S334ter-Rho) and mouse (C57 and T17M) retinas were obtained and fixed on polylysine-treated glass slides. Slides were warmed for 30 min at 37 °C and washed in 0.1 M PBS for 10 min three times. The antigen retrieval procedure was performed, using 10 mM citrate buffer. First, we placed the slides in the slide holder containing the citrate solution. The assembly was then placed in a 98 °C water bath for 30 min. Next, the slides were washed with 1× PBS twice for 10 min. Slides were kept in blocking buffer with 10% normal donkey serum and 0.3% Triton solution for 1 h at room temperature and washed with PBS three times. The sections were incubated with primary antibody (1:200) for NNAT (Abcam, Cambridge, MA, USA), Rhodopsin (B6), and peanut agglutinin lectin (PNA) with Fluorescein isothiocyanate (FITC) conjugate (Sigma, St. Louis, MO USA, 1:40) at 4 °C overnight. The slides were then washed three times with PBS and incubated with secondary antibody (1:1000) for 1 h at room temperature. After washing, the sides were cover slipped using a mounting medium containing 4′,6-diamidino-2-phenylindole (DAPI). Images were acquired using a wide-field fluorescence microscope (Carl Zeiss Axioplan2 Imaging microscope B000707, Carl Zeiss, Gottingen, Germany). Tree shrew and primate retinal sections were obtained from the laboratories of Dr. Norton and Dr. Gamlin, respectively, from the Vision Science Department at UAB. For the human retinal slides, the 55-year-old female donor was from BIOMAX, Inc. De-paraffinization of human retinal sections was performed before antigen retrieval and immunostaining.

Photoreceptor isolation

The isolation and culturing of primary rat photoreceptors were conducted using a protocol described previously (Shinde et al., 2016). The presence of rod photoreceptors and the absence of other retinal cell types in isolated cells were confirmed by qRT-PCR as described

in the study. The same protocol was used to isolate and culture mouse primary photoreceptor cells, extracting retinas from five mice. The petri dish for culture was coated with rod-specific Wheat germ and anti-wheat germ antibody in order to achieve photoreceptor-specific attachment.

Statistical analysis

Two-way analysis of variance (ANOVA) was used to determine the statistical significance of NNAT mRNA expression levels in SD and S334ter Rho retina, and one-way ANOVA was used to compare the protein expression of NNAT ($^{*}P<0.05$, $^{**}P<0.01$, $^{***}P<0.001$, $^{****}P<0.0001$). *T*-Test was used to analyze the fluorescence intensity for the primary cell culture immunostaining with NNAT.

Confocal imaging and analysis

We conducted IHC analysis with retinal sections and primary rod photoreceptor cells using anti-NNAT antibody. Confocal images were then taken to visualize the staining using the high-resolution 3D NIS element software imaging system.

RESULTS

NNAT is exclusively expressed in the outer segment (OS) of photoreceptors

Previous studies have demonstrated that NNAT is abundantly expressed in several organs, including the brain, pituitary gland, lungs, adrenal gland, uterus, skeletal muscle, ovaries, pancreas, and skin (Wijnholds et al., 1995; Niwa et al., 1997; Arava et al., 1999; John et al., 2001). The expression pattern of NNAT in different retinal cell types was examined using immunofluorescence microscopy in five different adult mammalian vertebrates, which included mice, rats, primates, tree shrews, and humans. We detected NNAT in all species; its immunoreactivity was predominantly restricted to the OS of WT photoreceptors without any evidence of staining in other retinal cell types (Fig. 1). High NNAT immunore-activity was identified in rodent (Fig. 1A–F in green and red), primate (Fig. 1G–I in green and red) and 55-year-old human (Fig. 1N in green) retinas. We also used the non-human primate retinal cryostat sections to perform the absorption control technique to confirm the specificity of the anti-NNAT antibody binding site (Fig. 1G). The left part of the image contains no staining for NNAT due to binding of the NNAT antibody with the human NNAT peptide. The antibody-peptide mixture was incubated for 30 min. The right part of the Fig. 1G contains the image obtained with immunohistochemically processed retinal sections. Compared to the previously mentioned rod-dominant retinas, relatively weak NNAT immunoreactivity was registered in the diurnal cone-dominant tree shrew's retinal sections (Fig. 1J–L). Tree shrew retinas are known to have rods constituted from 1% to 14% of the photoreceptor population, depending on retinal location (Muller and Peichl, 1989). Therefore, these results indicate that the NNAT immunoreactivity was not common between rod and cone photoreceptors.

It is interesting that NNAT was not detected in dendrites of other retinal neurons, as it has been observed in hippocampal neurons (Oyang et al., 2011). The only exception of altered NNAT intracellular localization was detected in RHO knockout retinas at P15. At this age, the $RHO^{-/-}$ mice already lost their OS. Therefore, we were not surprised to learn that NNAT

was detected mostly in the soma of photoreceptor cells and their synaptic terminals. Considering the difference in NNAT expression in the rod- and cone-dominant retinas, we next decided to specify the NNAT localization in the retinas.

NNAT is expressed in the rod but not in the cone photoreceptors

We performed the immunostaining of primate retinas with anti-NNAT antibody and PNA to label cones (Fig. 1H, I). Analysis of confocal images demonstrated non-significant co-localization of PNA and NNAT, suggesting that these cones are not the cell type that expresses NNAT. The 3D confocal images of primate retinas also confirmed our findings and collectively with the PNA-stained images indicated that it is unlikely that cone photoreceptors express NNAT. Because of a weak expression of NNAT in the diurnal tree shrew's retina (Fig. 1J), we next wondered whether NNAT is co-localized with rhodopsin. Using the B36 Rho antibody against rhodopsin and the NNAT antibody, we found that, like rhodopsin, NNAT is detected in rods (Fig. 1K, L). Confocal images of double-stained retinas demonstrated that while weak expression of rhodopsin in the tree shrew's retina was found in the inner segment and soma of rod photoreceptors (in red), the intercellular localization of NNAT (in green) was restricted to the OS of rods where their co-localization is shown as yellow-orange staining. Using Pearson's correlation coefficient, which represented the relationship between rhodopsin and NNAT staining in a single rod, we found that this correlation was positive for the tree shrew's and rat's rods (0.83 and 0.90, respectively). However, when we analyzed the PNA-stained cone of the primate retina, Pearson's correlation coefficient for PNA and NNAT was negative, suggesting that cone photoreceptors do not express NNAT.

We next isolated rat and mouse rod photoreceptor cells (n=5) and confirmed the NNAT expression by qRT-PCR and IHC analyses (Fig. 2A, B). The extracted RNA from isolated rods from SD rat retinas was converted to cDNA and qRT-PCR analysis was performed. As a result, both the whole retinal and the rod cell RNA extracts expressed NNAT, presenting additional evidence of the rod resident protein (Fig. 2A). The relative *NNAT* mRNA expression was twofold lower compared to the whole retinal RNA extract (P<0.001). Therefore, our data indicated that NNAT expression is limited to rod photoreceptors.

Expression and intracellular localization of NNAT are altered in retinas with ongoing stress

We demonstrated that NNAT is expressed in the rod's OS under normal physiological conditions. Therefore, we were curious to examine whether the localization and/or expression of NNAT is altered in degenerating retinas. Our interest was also fueled by the distribution of NNAT immunofluorescence in the $RHO^{-/-}$ mouse retinas, indicating potential changes in diseased retinas. Thus we isolated mouse primary photoreceptor cells and used retinal degenerative models of autosomal dominant retinitis pigmentosa (ADRP) expressing the rhodopsin transgene including the S334ter-4 Rho rats and T17M Rho mice (Fig. 1B, E) to test the hypothesis.

We treated isolated rod photoreceptor cells with the ER stress inducer, tunicamycin during 6 h and the performed IHC analysis with anti-NNAT antibody (Fig. 2B). Using confocal microscopy, we examined NNAT expression in rods in control and experimental groups and

found that the pattern of fluorescent labeling within the cell was not uniform. In stressed rod photoreceptors we observed more compact distribution of NNAT around the nucleus. In addition, the NNAT labeling within the nucleus was found in Tn-treated cells indicating that during the stress the NNAT could translocate to the nucleus.

Analyzing degenerating retinas, we found partial mislocalization of NNAT in the ONL of the retina compared to WT SD rat and C57BL6 mouse retinas (Fig. 1B, E). Rodent models of ADRP expressing S334ter, P23H and T17M rhodopsin experience severe retinal degeneration characterized by activated ER stress, oxidative stress, calcium dysregulation and mitochondrial dysfunction (Kunte et al., 2012; Shinde et al., 2012; Sizova et al., 2014). Taking this into account, we next tested a hypothesis that stress can alter NNAT expression in these photoreceptors. We observed a marked upregulation of NNAT mRNA in P30 and P40 S334ter Rho retinas compared to WT rats, demonstrating a correlation between ADRP progression and NNAT mRNA elevation (Fig. 2C). Thus, at P30, the difference was over twofold ($P<0.0001$), while at P60, the difference was 1.7-fold ($P<0.001$). Thus, qRT-PCR demonstrated an increase of NNAT in degenerating retinas. In addition to qRT-PCR, we run western blot with protein extracts isolated from S334ter and P23H RHO retinas. Finally, over 40- and 10-fold differences in NNAT expression were detected in S334ter and P23H RHO retinas, respectively as compared to SD retina suggesting that NNAT is responsive to the stress protein. Therefore, all together these results indicate that during the stress the NNAT can transport to the nucleus or accumulate around the nucleus without transporting to the OS and these events occur in addition to elevated expression of NNAT.

DISCUSSION

Here, for the first time, we assessed the distribution profile of NNAT in the retina and demonstrated that NNAT is present in the OS of rod photoreceptors. The retinal expression profile of NNAT was similar in all of the investigated mammalian retinas, which was indicative of a similar role of this protein across mammals. However, the pathophysiological conditions that can affect the intracellular localization of NNAT in rods and the consequences of the partial accumulation of NNAT are unclear. Although the precise function of NNAT remains unclear, it is thought to play a significant role in signal transduction and cell–cell communication in adult non-neuronal tissues and the developing central nervous system (Wijnholds et al., 1995). However, even though its expression was detected in other adult tissues, neither the expression nor localization of NNAT has been evaluated in the retina.

We identified NNAT in rod photoreceptors by protein (immunohistochemistry, western blot) and mRNA (qRT-PCR) expression analyses. However, the primary rod photoreceptor culture exhibits relatively lower NNAT expression level as compared to whole retina. This could be explained either by the fact that other retinal cell types also synthetize NNAT at low level undetectable by immunohistochemistry or by the stress that photoreceptors experience during their isolation and culturing. In favor of the latest hypothesis, stress-induced miRNA708 has been found to regulate expression of Nnat mRNA (Chitnis et al., 2013).

In vivo, the distribution of NNAT in health retinas is strictly limited by the OS of photoreceptors, the cellular department of photoreceptors where absorbed light is converted into electrical signals that are transmitted to the brain (Cervetto and Piccolino, 1982). The biochemical process of phototransduction in rod and cone photoreceptors is relatively similar (Miller et al., 1994), and therefore rules out the possibility of the involvement of NNAT in the biochemical cascade of phototransduction. On the other hand, there is a difference between rod and cone disk membrane structure. In rods, disk membranes are physically separate from the plasma membrane, whereas the cone disks remain as folding of the plasma membrane. Because NNAT is proposed to be a membrane protein (Joseph et al., 1994, 1995), it is possible that its role in the OS of adult rods is related to the maintenance of the rod disk membrane's structural integrity. The overexpression and partial mislocalization of NNAT has been identified in ADRP retina (Figs. 1 and 2). Knowing that NNAT has a strong tendency to misfold and form cellular inclusions driving apoptotic cell death (Joseph, 2014), it is not surprising that the rodent ADRP models, experiencing severe cellular stress and apoptotic photoreceptor cell death (Kunte et al., 2012; Shinde et al., 2012) demonstrate partial accumulation of NNAT in the ONL of the retina. Possibly, the observed partial retention of NNAT is due to its ability to regulate Ca^{2+} signaling and antagonize the SERCA2b pump (Sharma et al., 2013). Thus, in our previous study, we have found that both the aberrant Ca^{2+} signaling and compromised SERCA2b activity were detected in S334ter and P23H RHO transgenic retinas (Shinde et al., 2016). In another retinal degenerative model, a rhodopsin knockout mouse, the altered Nnat localization was detected as well. However, compared to previous models, the NNAT is localized at the synaptic terminal of photoreceptors. The *in vivo* data coincide with the results obtained with primary photoreceptor culture demonstrating accumulation of the NNAT around and within the nucleus during the stress. Together these findings indicate the mobility of NNAT distribution in healthy and diseased retinas. Besides the distribution, rod photoreceptor can respond to the stress by an increase in NNAT expression. A notable elevation of NNAT was found in transgenic S334ter RHO-4 retinas that are known to have activation of the ER stress response already at P12 (Shinde et al., 2012) and degenerate faster as compared to P23H RHO-3 mice. This implies that stress degree can determine the level of NNAT expression in photoreceptors. Our finding with rat models of retinitis pigmentosa correlates with the data obtained with fibroblasts isolated from patients with Leber congenital amaurosis (LCA), in that NNAT was found to be up-regulated (Lustremant et al., 2013). This fact provides a link between activated ER stress response contributing to the pathogenesis of the LCA (Zhang et al., 2012) and over-expression of NNAT. Together the literature describing phenomenon of NNAT aggregation in Lafora bodies (Sharma et al., 2013; Joseph, 2014) and alteration of NNAT expression during ER stress condition (Vrang et al., 2010) both support our findings of mislocalized NNAT in degenerating retina with ongoing ER stress. We speculate that there is only partial translocation of NNAT from the inner segment (ER) to the OS thus resulting in nuclear accumulation in the ONL, as seen in other disease models.

In summary, our study is the foremost to demonstrate that NNAT is exclusively expressed in rod photoreceptors of mammalian retinas. However, given that different NNAT isoforms are expressed in rats and mice, neither individual isoform expression nor their individual roles in the developing or adult healthy and diseased retinas have been investigated. This study

highlights the need for further investigations of NNAT in the retina using photoreceptor-specific NNAT KO models to establish the precise role of NNAT in developing and adult photoreceptors as well as in healthy and diseased retinas.

Acknowledgments

SOURCES OF FUNDING

This work was supported by the NEI R01EY020905 grant and the VSRC Core Grant P30 EY003039.

Abbreviations

ADRP	autosomal dominant retinitis pigmentosa
ANOVA	analysis of variance
ER	endoplasmic reticulum
LCA	Leber congenital amaurosis
NNAT	neuronatin
OS	outer segment
P	postnatal day
PBS	phosphate-buffered saline
PNA	peanut agglutinin lectin
qRT-PCR	quantitative real time polymerase chain reaction
SD	Sprague–Dawley
WT	wild-type

References

Arava Y, Adamsky K, Ezerzer C, Ablamunits V, Walker MD. Specific gene expression in pancreatic beta-cells: cloning and characterization of differentially expressed genes. Diabetes. 1999; 48:552–556. [PubMed: 10078555]

Cervetto L, Piccolino M. Processing of visual signals in vertebrate photoreceptors. Arch Ital Biol. 1982; 120:242–270. [PubMed: 6291477]

Chitnis N, Pytel D, Diehl JA. UPR-inducible miRNAs contribute to stressful situations. Trends Biochem Sci. 2013; 38:447–452. [PubMed: 23906563]

Chu K, Tsai MJ. Neuronatin, a downstream target of BETA2/NeuroD1 in the pancreas, is involved in glucose-mediated insulin secretion. Diabetes. 2005; 54:1064–1073. [PubMed: 15793245]

Dorrell MI, Aguilar E, Weber C, Friedlander M. Global gene expression analysis of the developing postnatal mouse retina. Invest Ophthalmol Vis Sci. 2004; 45:1009–1019. [PubMed: 14985324]

Dou D, Joseph R. Cloning of human neuronatin gene and its localization to chromosome-20q 11.2-12: the deduced protein is a novel ‘proteolipid’. Brain Res. 1996; 723:8–22. [PubMed: 8813377]

Dugu L, Takahara M, Tsuji G, Iwashita Y, Liu X, Furue M. Abundant expression of neuronatin in normal eccrine, apocrine and sebaceous glands and their neoplasms. J Dermatol. 2010; 37:846–848. [PubMed: 20883377]

Joe MK, Lee HJ, Suh YH, Han KL, Lim JH, Song J, Seong JK, Jung MH. Crucial roles of neuronatin in insulin secretion and high glucose-induced apoptosis in pancreatic beta-cells. Cell Signal. 2008; 20:907–915. [PubMed: 18289831]

John RM, Aparicio SA, Ainscough JF, Arney KL, Khosla S, Hawker K, Hilton KJ, Barton SC, Surani MA. Imprinted expression of neuronatin from modified BAC transgenes reveals regulation by distinct and distant enhancers. Dev Biol. 2001; 236:387–399. [PubMed: 11476579]

Joseph RM. Neuronatin gene: imprinted and misfolded: studies in Lafora disease, diabetes and cancer may implicate NNAT-aggregates as a common downstream participant in neuronal loss. Genomics. 2014; 103:183–188. [PubMed: 24345642]

Joseph R, Dou D, Tsang W. Molecular cloning of a novel mRNA (neuronatin) that is highly expressed in neonatal mammalian brain. Biochem Biophys Res Commun. 1994; 201:1227–1234. [PubMed: 8024565]

Joseph R, Dou D, Tsang W. Neuronatin mRNA: alternatively spliced forms of a novel brain-specific mammalian developmental gene. Brain Res. 1995; 690:92–98. [PubMed: 7496812]

Kunte MM, Choudhury S, Manheim JF, Shinde VM, Miura M, Chiodo VA, Hauswirth WW, Gorbatyuk OS, Gorbatyuk MS. ER stress is involved in T17M rhodopsin-induced retinal degeneration. Invest Ophthalmol Vis Sci. 2012; 53:3792–3800. [PubMed: 22589437]

Lustremant C, Habeler W, Plancheron A, Goureau O, Grenot L, de la Grange P, Audo I, Nandrot EF, Monville C. Human induced pluripotent stem cells as a tool to model a form of Leber congenital amaurosis. Cell Reprogram. 2013; 15:233–246. [PubMed: 23663011]

Miller JL, Picones A, Korenbrot JI. Differences in transduction between rod and cone photoreceptors: an exploration of the role of calcium homeostasis. Curr Opin Neurobiol. 1994; 4:488–495. [PubMed: 7812136]

Muller B, Peichl L. Topography of cones and rods in the tree shrew retina. J Comp Neurol. 1989; 282:581–594. [PubMed: 2723153]

Mzhavia N, Yu S, Ikeda S, Chu TT, Goldberg I, Dansky HM. Neuronatin: a new inflammation gene expressed on the aortic endothelium of diabetic mice. Diabetes. 2008; 57:2774–2783. [PubMed: 18591389]

Niwa H, Harrison LC, DeAizpurua HJ, Cram DS. Identification of pancreatic beta cell-related genes by representational difference analysis. Endocrinology. 1997; 138:1419–1426. [PubMed: 9075697]

Oyang EL, Davidson BC, Lee W, Poon MM. Functional characterization of the dendritically localized mRNA neuronatin in hippocampal neurons. PLoS One. 2011; 6:e24879. [PubMed: 21935485]

Poon MM, Choi SH, Jamieson CA, Geschwind DH, Martin KC. Identification of process-localized mRNAs from cultured rodent hippocampal neurons. J Neurosci. 2006; 26:13390–13399. [PubMed: 17182790]

Sharma J, Mukherjee D, Rao SN, Iyengar S, Shankar SK, Satishchandra P, Jana NR. Neuronatin-mediated aberrant calcium signaling and endoplasmic reticulum stress underlie neuropathology in Lafora disease. J Biol Chem. 2013; 288:9482–9490. [PubMed: 23408434]

Shinde VM, Sizova OS, Lin JH, LaVail MM, Gorbatyuk MS. ER stress in retinal degeneration in S334ter Rho rats. PLoS One. 2012; 7:e33266. [PubMed: 22432009]

Shinde V, Kotla P, Strang C, Gorbatyuk M. Unfolded protein response-induced dysregulation of calcium homeostasis promotes retinal degeneration in rat models of autosomal dominant retinitis pigmentosa. Cell Death Dis. 2016; 7:e2085. [PubMed: 26844699]

Siu IM, Bai R, Gallia GL, Edwards JB, Tyler BM, Eberhart CG, Riggins GJ. Coexpression of neuronatin splice forms promotes medulloblastoma growth. Neuro Oncol. 2008; 10:716–724. [PubMed: 18701710]

Sizova OS, Shinde VM, Lenox AR, Gorbatyuk MS. Modulation of cellular signaling pathways in P23H rhodopsin photoreceptors. Cell Signal. 2014; 26:665–672. [PubMed: 24378535]

Suh YH, Kim WH, Moon C, Hong YH, Eun SY, Lim JH, Choi JS, Song J, Jung MH. Ectopic expression of Neuronatin potentiates adipogenesis through enhanced phosphorylation of cAMP-response element-binding protein in 3T3-L1 cells. Biochem Biophys Res Commun. 2005; 337:481–489. [PubMed: 16223607]

Usui H, Ichikawa T, Miyazaki Y, Nagai S, Kumanishi T. Isolation of cDNA clones of the rat mRNAs expressed preferentially in the prenatal stages of brain development. Brain Res Dev Brain Res. 1996; 97:185–193. [PubMed: 8997503]

Vrang N, Meyre D, Froguel P, Jelsing J, Tang-Christensen M, Vatin V, Mikkelsen JD, Thirstrup K, Larsen LK, Cullberg KB, Fahrenkrug J, Jacobson P, Sjostrom L, Carlsson LM, Liu Y, Liu X, Deng

HW, Larsen PJ. The imprinted gene neuronatin is regulated by metabolic status and associated with obesity. Obesity (Silver Spring). 2010; 18:1289–1296. [PubMed: 19851307]

Wijnholds J, Chowdhury K, Wehr R, Gruss P. Segment-specific expression of the neuronatin gene during early hindbrain development. Dev Biol. 1995; 171:73–84. [PubMed: 7556909]

Xu DS, Yang C, Proescholdt M, Brundl E, Brawanski A, Fang X, Lee CS, Weil RJ, Zhuang Z, Lonser RR. Neuronatin in a subset of glioblastoma multiforme tumor progenitor cells is associated with increased cell proliferation and shorter patient survival. PLoS One. 2012; 7:e37811. [PubMed: 22624064]

Yang J, Wei J, Wu Y, Wang Z, Guo Y, Lee P, Li X. Metformin induces ER stress-dependent apoptosis through miR-708-5p/NNAT pathway in prostate cancer. Oncogenesis. 2015; 4:e158. [PubMed: 26075749]

Zhang T, Baehr W, Fu Y. Chemical chaperone TUDCA preserves cone photoreceptors in a mouse model of Leber congenital amaurosis. Invest Ophthalmol Vis Sci. 2012; 53:3349–3356. [PubMed: 22531707]

Zheng S, Chou AH, Jimenez AL, Khodadadi O, Son S, Melega WP, Howard BD. The fetal and neonatal brain protein neuronatin protects PC12 cells against certain types of toxic insult. Brain Res Dev Brain Res. 2002; 136:101–110. [PubMed: 12101027]

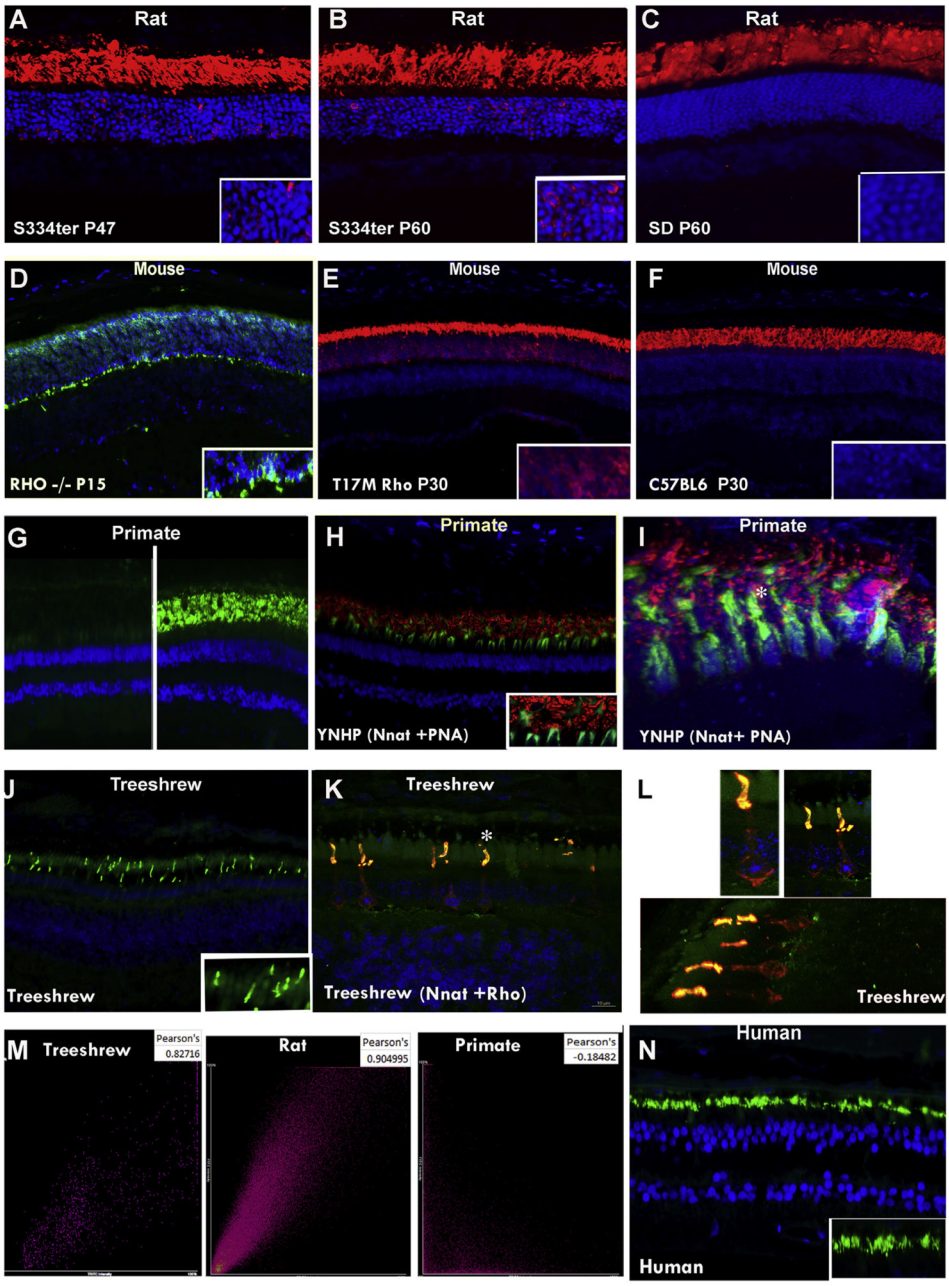

Fig. 1.

Neuronatin (NNAT) expression in the mammalian retina detected by immunohistochemical analysis. (A–C) NNAT immunolabeling was detected in the OS of photoreceptors in the rat transgenic S334ter rhodopsin and wild-type Sprague–Dawley retinas at P47, P60 and P60, respectively (in red). DAPI was used to stain nuclei of the retina and visualize the ONL of the retina (in blue). In transgenic retinas (A, B), we observed partial intracellular mislocalization of NNAT from the OS to the soma of photoreceptor cells, while in the SD retina the detection of NNAT was restricted to the OS (C). (D–F): NNAT immunolabeling was observed in the mouse transgenic rhodopsin knockout, T17M rhodopsin, and the wild-

type C57BL6 retinas at P15, P30 and P30, respectively. (D) In the $RHO^{-/-}$ retina, NNAT was detected predominantly at synaptic terminals and in the soma of photoreceptors (in green) while its accumulation in T17M rhodopsin retinas (in red) was partially observed in the soma (E). In C57BL6 retinas, NNAT immunolabeling was limited to the OS of photoreceptors (in red). (G–I) NNAT expression in the OS of the non-human primate (NHP; female, 12 years old) retinas. (G) NNAT was detected in the OS of primate photoreceptors. We applied the absorption technique to verify the specificity of antibodies against the NNAT protein (see details in the text). Control immunolabeling (left) showed no staining of NNAT, while the experimental primate retina (right) demonstrated NNAT immunolabeling (in green). (H, I) Detection of NNAT in the primate retina with the peanut agglutinin (PNA)-FITC conjugated antibody used to label cones (in green). (H) Immunolabeling of NNAT (in red) did not co-localize with labeled cones in the primate retina. (I) 3D confocal images taken with primate retinas stained with anti-NNAT antibody (in red) and the PNA (in green). (J–L) NNAT immunolabeling was observed in the cone-dominant tree shrew retinas. Immunostaining of tree shrew retinas with antibodies against rhodopsin (in red) and NNAT (in green) resulted in their overlapping, detected in yellow by confocal microscopy, in rods (K and L). (L) Immunolabeling of rhodopsin did not overlap with NNAT immunolabeling in the inner segments of rod photoreceptors (in red). (M) A single tree shrew rod photoreceptor cell labeled with an asterisk on image K, and a rat photoreceptor cell, and cone photoreceptor cell, labeled with asterisks on image I, were used for the graphical representation of the rhodopsin+NNAT co-localization detected by Pear's coefficient. This coefficient was positive in the tree shrew and rat rod photoreceptors and was negative for the primate single cone. (N) Expression of the NNAT protein in the OS of the human retina (female, 55 years old, in green). (For interpretation of the references to colour in this figure legend, the reader is referred to the web version of this article.)

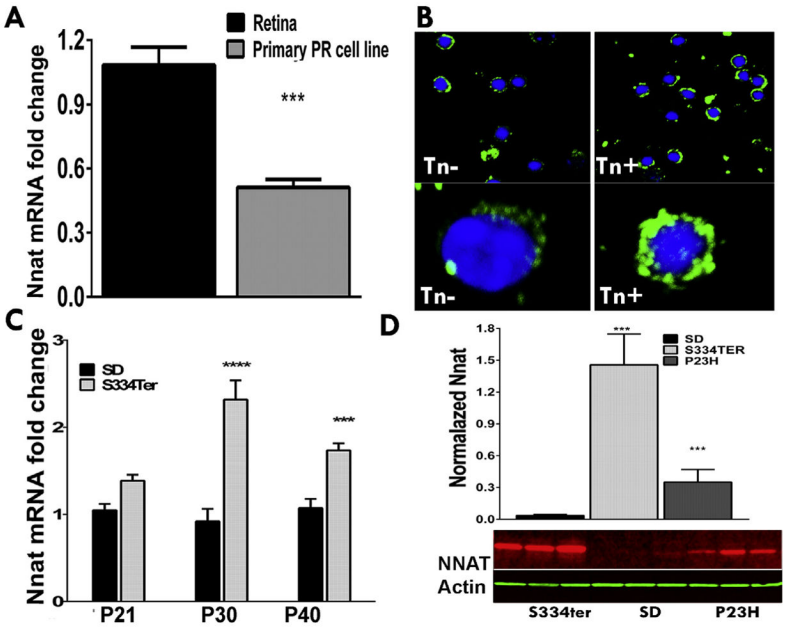

Fig. 2.

NNAT expression in the mammalian retina detected by qRT-PCR, immunohistochemical and western blot analyses. (A) NNAT mRNA expression estimated by the qPCR analysis in the wild-type rat whole retina and isolated rod cells. (B) Detection of NNAT in isolated mouse photoreceptors. Cells were treated with ER stress inducer, tunicamycin (Tn) as described above. Accumulation of NNAT around and within the nucleus was detected in Tn-treated (Tn^{+}) as compared to untreated (Tn^{-}) cells. Bottom panel: 100 × 3D images of the randomly selected control and Tn- treated cells. (C) Expression of NNAT mRNA in the wild-type (SD) and S334ter retina at the P21, P30, P40 timeline detected by qRT-PCR. (D) Western blot quantification for NNAT protein in the wild-type, S334ter and P23H retinas. Bottom panel: Western blot image detecting increase in NNAT in retinal extracts of two transgenic rat models of ADRP (S334ter and P23H rhodopsin) as compared to SD.